3 Methods for Band Structure Calculations in Solids

A. Ernst[1] and M. Lüders[2]

[1] Max-Planck-Institut für Mikrostrukturphysik, Weinberg 2, 06120 Halle, Germany
[2] Daresbury Laboratory, Warrington WA4 4AD, United Kingdom

Abstract. The calculation of the ground-state and excited-state properties of materials is one of the main goals of condensed matter physics. While the most successful first-principles method, the density-functional theory (DFT), provides, in principle, the exact ground-state properties, the many-body method is the most suitable approach for studying excited-state properties of extended systems. Here we discuss general aspects of the Green's function and different approximations for the self-energy to solve the Dyson equation. Further we present some tools for solving the Dyson equation with several approximations for the self-energy: a highly precise combined basis method providing the band structure in the Kohn-Sham approximation, and some implementations for the random-phase approximation.

3.1 The Green's Function and the Many-Body Method

3.1.1 General Considerations

The Green's function is a powerful tool for studying ground state and excited state properties of condensed matter. The basic idea of the Green's function has its origin in the theory of differential equations. The solution of any inhomogeneous differential equation with a Hermitian differential operator $\hat{H}$, a complex parameter z, and a given source function $u(\boldsymbol{r})$ of the form

$$\left[z - \hat{H}(\boldsymbol{r})\right] \psi(\boldsymbol{r}) = u(\boldsymbol{r}) \tag{3.1}$$

can be represented as an integral equation

$$\psi(\boldsymbol{r}) = \varphi(\boldsymbol{r}) + \int G(\boldsymbol{r}, \boldsymbol{r}'; z) u(\boldsymbol{r}') \mathrm{d}^3 r'. \tag{3.2}$$

Here the so-called Green's function $G(\boldsymbol{r}, \boldsymbol{r}'; z)$ is a coordinate representation of the resolvent of the differential operator $\hat{H}$, i.e. $\hat{G} = [z - \hat{H}]^{-1}$, which obeys the differential equation

$$\left[z - \hat{H}(\boldsymbol{r})\right] G(\boldsymbol{r}, \boldsymbol{r}'; z) = \delta(\boldsymbol{r} - \boldsymbol{r}'), \tag{3.3}$$

and the function $\varphi(\boldsymbol{r})$ is a general solution of the homogeneous equation associated with (3.1), i.e. for $u(\boldsymbol{r}) = 0$. The integral equation (3.2) contains, in

A. Ernst and M. Lüders, Methods for Band Structure Calculations in Solids, Lect. Notes Phys. **642**, 23–54 (2004)
http://www.springerlink.com/

contrast to the differential equation (3.1), also information about the boundary conditions, which are built into the function $\varphi(\boldsymbol{r})$. This method is in many cases very convenient and widely used in many-body physics. In this review we shall consider the application of the Green's function method in condensed matter physics at zero temperature. The formalism can be generalised to finite temperatures but this is beyond the scope of this papers and can be found in standard textbooks [3.22, 3.42, 3.24]

The evolution of an N-body system is determined by the time-dependent Schrödinger equation (atomic units are used throughout)

$$i\frac{d\Psi(t)}{dt} = \hat{H}\Psi(t), \tag{3.4}$$

where $\Psi(t) \equiv \Psi(\boldsymbol{r}_1, \boldsymbol{r}_2, ..., \boldsymbol{r}_N; t)$ is a wave function of the system and $\hat{H}$ is the many-body Hamiltonian

$$\hat{H} = \hat{H}_0 + \hat{V}, \tag{3.5}$$

which includes the kinetic energy and the external potential

$$\hat{H}_0 = -\sum_i \frac{\nabla_i^2}{2} + \sum_i v_{\text{ext}}(\boldsymbol{r}_i), \tag{3.6}$$

and the interactions between the particles

$$\hat{V} = \frac{1}{2}\sum_{i,j} \frac{1}{|\boldsymbol{r}_i - \boldsymbol{r}_j|}. \tag{3.7}$$

Knowing the wave function $\Psi(t)$, the average value of any operator $\hat{A}$ can be obtained from the equation:

$$\mathcal{A}(t) = \langle \Psi^*(t)\hat{A}\Psi(t)\rangle \ . \tag{3.8}$$

The many-body wave function can be expanded in a complete set of time-independent either anti-symmetrized (for fermions) or symmetrized (for bosons) products of single particle wave-functions: $\Phi_{i_1,\ldots,i_n}(\boldsymbol{r}_1, \ldots, \boldsymbol{r}_N)$

$$\Psi(\boldsymbol{r}_1, \boldsymbol{r}_2, ..\boldsymbol{r}_N; t) = \sum_{\{i_1,i_2,\ldots,i_N\}} C_{\{i_1,i_2,\ldots,i_N\}}(t)\, \Phi_{i_1,\ldots,i_n}(\boldsymbol{r}_1, \ldots, \boldsymbol{r}_N). \tag{3.9}$$

These (anti-) symmetrized products of single-particle states $\phi_i(\boldsymbol{r})$ are given by

$$\Phi_{i_1,\ldots,i_n}(\boldsymbol{r}_1, \ldots, \boldsymbol{r}_N) = \sum_{\mathcal{P}} (\pm 1)^{\mathcal{P}} \phi_{\mathcal{P}(i_1)}(\boldsymbol{r}_1)\phi_{\mathcal{P}(i_2)}(\boldsymbol{r_2})...\phi_{\mathcal{P}(i_N)}(\boldsymbol{r}_N) \tag{3.10}$$

where $\mathcal{P}$ denotes all permutations of the indices $i_1, \ldots, i_N$ and $(-1)^{\mathcal{P}}$ yields a minus sign for odd permutations. In case of Fermions this anti-symmetrized

product can conveniently be written as a determinant, the so-called Slater determinant,

$$\Phi_{i_1,\ldots,i_n}(\boldsymbol{r}_1,\ldots,\boldsymbol{r}_N) = |\phi_{i_1}(\boldsymbol{r}_1),\phi_{i_2}(\boldsymbol{r_2}),\ldots\phi_{i_N}(\boldsymbol{r}_N)|, \tag{3.11}$$

which already fulfills Pauli's exclusion principle. The basis set can be arbitrary, but in practice one uses functions which are adequate for the particlar problem. For example, the plane wave basis is appropriate for the description of a system with free or nearly free electrons. Systems with localised electrons are usually better described by atomic-like functions. For systems with a large number of particles solving equation (3.4) using the basis expansion (3.9) is a quite formidable task.

To describe a many-body system one can use the so-called second quantisation: instead of giving a complete wave function one specifies the numbers of particles to be found in the one-particle states $\phi_1(\boldsymbol{r}), \phi_2(\boldsymbol{r}), .., \phi_N(\boldsymbol{r})$. As a result the many-body wave function is defined by the expansion coefficients at the occupation numbers and the Hamiltonian, as well as any other operator can be expressed in terms of the so-called creation and annihilation operators $\hat{c}_i^+$ and $\hat{c}_i$, obeying certain commutation or anticommutation relations according to the statistical properties of the particles (fermions or bosons). The creation operator $\hat{c}_i^+$ increases the number of particles by one, while the annihilation operators $\hat{c}_i$ decreases the occupation number of a state by one. Any observable can be represented as some combination of these operators. For example, a one-particle operator $\hat{A}$ can be expressed as

$$\hat{A} = \sum_{i,k} A_{ik}\hat{c}_i^+\hat{c}_k, \tag{3.12}$$

where A_{ik} are matrix elements of $\hat{A}$. Often it is convenient to use the field operators [1]

$$\begin{aligned}\hat{\psi}_\sigma^+(\boldsymbol{r}) &= \sum_i \phi_{i\sigma}(\boldsymbol{r})\hat{c}_{i\sigma}^+ \\ \hat{\psi}_\sigma(\boldsymbol{r}) &= \sum_i \phi_{i\sigma}(\boldsymbol{r})\hat{c}_{i\sigma}\ ,\end{aligned} \tag{3.13}$$

which can be interpreted as creation and annihilation operators of a particle with spin σ at a given point $\boldsymbol{r}$. In this representation a single particle operator is given as

$$\hat{A} = \sum_\sigma \int \mathrm{d}^3 r \hat{\psi}_\sigma^+(\boldsymbol{r})\hat{A}\hat{\psi}_\sigma(\boldsymbol{r}), \tag{3.14}$$

[1] Here we have explicitly included the spin-indices. In the remainder of the paper, we include the spin in the other quantum numbers, wherever not specified explicitly

where A is of the same form as the operator $\hat{A}$ in first quantisation, but without coordinates and momenta beeing operators.

Suppose we have a system with N particles in the ground state, which is defined by the exact ground state wave function Ψ_0. If at time $t_0 = 0$ a particle with quantum number i is added into the system, the system is described by $c_i^+|\Psi_0\rangle$. The evolution of the system in time will now proceed according to $e^{-i\hat{H}(t-t_0)}c_i^+|\Psi_0\rangle$. The probability amplitude for finding the added particle in the state j, is the scalar product of $e^{-i\hat{H}(t-t_0)}c_i^+|\Psi_0\rangle$ with the function $c_j^+e^{-i\hat{H}(t-t_0)}|\Psi_0\rangle$, describing a particle in the state j, added to the ground state at time t. The resulting probability amplitude is given by $\langle\Psi_0|e^{i\hat{H}(t-t_0)}c_je^{-i\hat{H}(t-t_0)}c_i^+|\Psi_0\rangle$. Analogously, a particle removed from a state can be described with the function $\pm\langle\Psi_0|e^{-i\hat{H}(t-t_0)}c_i^+e^{i\hat{H}(t-t_0)}c_j|\Psi_0\rangle$, where plus sign applies to Bose statistics and minus sign to Fermi statistics. Both processes contribute to the definition of the one-particle causal Green's function:

$$G(j,t;i,t_0) = -i\langle\Psi_0|T\left[\hat{c}_j(t)\hat{c}_i^+(t_0)\right]|\Psi_0\rangle. \tag{3.15}$$

Here we have used Heisenberg representation of the operators $\hat{c}_i$ and $\hat{c}_i^+$:

$$\hat{c}_i(t) = e^{i\hat{H}t}\hat{c}_ie^{-i\hat{H}t}\ . \tag{3.16}$$

The symbol T (3.15) is Wick's time-ordering operator which rearranges a product of two time-dependent operators so that the operator referring to the later time appears always on the left:

$$T\left[\hat{c}_j(t)\hat{c}_i^+(t_0)\right] = \begin{cases} \hat{c}_j(t)\hat{c}_i^+(t_0) & (t > t_0) \\ \pm\hat{c}_i^+(t_0)\hat{c}_j(t) & (t < t_0) \end{cases}\ . \tag{3.17}$$

The physical meaning of the Green's function in this representation is that for $t > t_0$ $G(i,t_0;j,t)$ describes the propagation of a particle created at time t_0 in the state i and detected at time t in the state j. For $t < t_0$, the Green's function describes the propagation of a hole in the state j emitted at time t into the state i at time t_0. Analogously to the above, one can write down the Green's function in the space-time representation:

$$G(\boldsymbol{r}_0,t_0;\boldsymbol{r},t) = -i\langle\Psi_0|T\left[\hat{\psi}(\boldsymbol{r}_0,t_0)\hat{\psi}^+(\boldsymbol{r},t)\right]|\Psi_0\rangle, \tag{3.18}$$

where $\hat{\psi}(\boldsymbol{r},t)$ and $\hat{\psi}^+(\boldsymbol{r},t)$ are particle annihilation and creation operators in the Heisenberg representation.

The time-evolution of the Green's function is controlled by the equation of motion. For $V = 0$ this is reduced to

$$\left(i\frac{\partial}{\partial t} - \hat{H}(\boldsymbol{r})\right)G(\boldsymbol{r}t,\boldsymbol{r}'t') = \delta(\boldsymbol{r}-\boldsymbol{r}')\delta(t-t'), \tag{3.19}$$

which follows directly from the equation of motion of the field operators:

$$i\frac{\partial\hat{\psi}(\boldsymbol{r},t)}{\partial t} = \left[\hat{\psi}(\boldsymbol{r},t),\hat{H}\right], \tag{3.20}$$

and a similar equation for the creation operator $\hat{\psi}^{+}(\boldsymbol{r},t)$. Taking the Fourier transform of (3.19) into frequency space, we get

$$\left[\omega - \hat{H}(\boldsymbol{r})\right] G(\boldsymbol{r},\boldsymbol{r}';\omega) = \delta(\boldsymbol{r}-\boldsymbol{r}'), \tag{3.21}$$

which demonstrates, that $G(\boldsymbol{r},\boldsymbol{r'};\omega)$ is a Green's function in the mathematical sence, as described above in (3.3).

The one-particle Green's function has some important properties which make the use of the Green's function method in condensed matter physics attractive. The Green's function contains a great deal of information about the system: knowing the single-particle Green's function, one can calculate the ground state expectation value of any single-particle operator:

$$\mathcal{A}(t) = \pm i \int \left[\lim_{t'\to t+0}\lim_{\boldsymbol{r}'\to\boldsymbol{r}} \hat{A}(\boldsymbol{r})\, G(\boldsymbol{r},t;\boldsymbol{r}',t')\right] \mathrm{d}^3 r. \tag{3.22}$$

As a consequence, in particular, the charge density and the total energy can be found for any system in the ground state at zero temperature. Furthermore the one-particle Green's function describes single-particle excitations. In what follows, we shall discuss the latter in more detail.

For simplicity, in the following paragraphs we consider the homogeneous electron gas. Due to the translational invariance, the momentum $\boldsymbol{k}$ is a good quantum number, and we can use the basis functions $\phi_{\boldsymbol{k}}(\boldsymbol{r}) = \frac{1}{\sqrt{N}} e^{i\boldsymbol{k}\cdot\boldsymbol{r}}$. It can easily be verified that the Green's function of the homogeneous electron gas is diagonal in momentum space and depends only on the time difference:

$$G(\boldsymbol{k}t,\boldsymbol{k}'t') = \delta_{\boldsymbol{k},\boldsymbol{k}'} G(\boldsymbol{k},t-t') \tag{3.23}$$

The time-ordering operator T can be mathematically expressed using the Heaviside function $\theta(t)$, which leads to the following equation for the Green's function

$$\begin{aligned} iG_{\boldsymbol{k}}(t-t') = {} & \theta(t-t') \sum_n e^{-i\left[E_n^{N+1}-E_0^N\right](t-t')} |\langle N+1,n|c_{\boldsymbol{k}}^{+}|N,0\rangle|^2 \\ & \pm\theta(t'-t) \sum_n e^{-i\left[E_0^N-E_n^{N-1}\right](t-t')} |\langle N-1,n|c_{\boldsymbol{k}}|N,0\rangle|^2 \,. \end{aligned} \tag{3.24}$$

Here E_n^{N+1} and E_n^{N-1} are all the exact eigenvalues of the $N+1$ and $N-1$ particle systems respectively, n represents all quantum numbers necessary to specify the state completely, and E_0^N is the exact ground state energy for the system with N particles ($n=0$). Using the integral form of the Heaviside function,

$$\theta(t) = -\lim_{\Gamma\to 0}\frac{1}{2\pi i}\int\limits_{-\infty}^{\infty}\frac{e^{-i\omega t}}{\omega + i\Gamma}, \tag{3.25}$$

the Green's function can easily be Fourier transformed into the frequency representation:

$$G_{\boldsymbol{k}}(\omega) = \lim_{\Gamma\to 0}\left[\sum_n \frac{|\langle N+1,n|c^+_{\boldsymbol{k}}|N,0\rangle|^2}{\omega - \left[E^{N+1}_n - E^N_0\right] + i\Gamma}\right.$$
$$\left. \mp \sum_n \frac{|\langle N-1,n|c_{\boldsymbol{k}}|N,0\rangle|^2}{\omega - \left[E^N_0 - E^{N-1}_n\right] - i\Gamma}\right]. \tag{3.26}$$

Equation (3.26) provides insight into the analytical properties of the single-particle Green's function. The frequency ω appears only in the denominators of the above equation. The Green's function is a meromorphic function of the complex variable ω, and all its singularities are simple poles, which are infinitesimally shifted into the upper half-plane of ω when $\omega > 0$ and into the lower one if $\omega < 0$. Each pole corresponds to an excitation energy. If we now set

$$E^{N+1}_n - E^N_0 = (E^{N+1}_n - E^{N+1}_0) + (E^{N+1}_0 - E^N_0) = \omega_n - \mu$$
$$E^{N-1}_n - E^N_0 = (E^{N-1}_n - E^{N-1}_0) + (E^{N-1}_0 - E^N_0) = \mu' - \omega'_n, \tag{3.27}$$

then ω_n and ω'_n denote excitation energies in the $(N+1)$-and $(N-1)$-particle systems respectively and μ and μ' are changes of the ground state energy when a particle is added to the N-particle system or otherwise is removed from the N-particle system, , known as the chemical potentials. In the thermodynamic limit ($N\to\infty, V\to\infty, N/V = \text{const}$) one finds within an error of the order N^{-1} that the chemical potential and the excitation energies are independent of the particle number, i.e.

$$\omega_n \approx \omega'_n\ , \quad \mu \approx \mu'\ .$$

Another simple property of the Green's function which follows from (3.26) is the asymptotic behaviour for large $|\omega|$:

$$G_{\boldsymbol{k}}(\omega) \sim \frac{1}{\omega}. \tag{3.28}$$

It is convenient to introduce the spectral densities:

$$A^+_{\boldsymbol{k}}(\epsilon) = \sum_n |\langle N+1,n|c^+_{\boldsymbol{k}}|N,0\rangle|^2\delta(\epsilon-\omega_n) \tag{3.29 a}$$

$$A^-_{\boldsymbol{k}}(\epsilon) = \sum_n |\langle N-1,n|c_{\boldsymbol{k}}|N,0\rangle|^2\delta(\epsilon-\omega_n), \tag{3.29 b}$$

which are real and positive functions, and whose physical interpretation is simple. The spectral density function $A^+_{\boldsymbol{k}}(\omega)$ gives the probability that the original N-particle system with a particle added into the state $\boldsymbol{k}$ will be found in an exact eigenstate of the $(N+1)$-particle system. In other words, it counts the number of states with excitation energy ω and momentum $\boldsymbol{k}$ which are connected to the ground state through the addition of an extra particle. Similarly, the function $A^-_{\boldsymbol{k}}(\omega)$ is the probability that the original N-particle system and a hole will be found at an exact eigenstate of the $(N-1)$-particle system. Using the spectral functions (3.29), we may write the causal Green's function (3.26) in the Lehmann representation:

$$G_{\boldsymbol{k}}(\omega) = \lim_{\Gamma\to 0} \int_0^\infty \mathrm{d}\epsilon \left[\frac{A^+_{\boldsymbol{k}}(\epsilon)}{\omega - (\epsilon+\mu) + i\Gamma} \mp \sum_n \frac{A^-_{\boldsymbol{k}}(\epsilon)}{\omega + \epsilon - \mu - i\Gamma} \right]. \quad (3.30)$$

In addition, the spectral functions (3.29) may by expressed via the causal Green's function (3.26):

$$A^+_{\boldsymbol{k}}(\omega-\mu) = -\frac{1}{\pi}\mathrm{Im}\, G_{\boldsymbol{k}}(\omega), \quad \omega > \mu \quad (3.31\text{ a})$$

$$A^-_{\boldsymbol{k}}(\mu-\omega) = \pm\frac{1}{\pi}\mathrm{Im}\, G_{\boldsymbol{k}}(\omega), \quad \omega < \mu \quad (3.31\text{ b})$$

3.1.2 Quasi-Particles

From the Lehmann representation of the Green's function (3.30), it easy to see that the special features of the Green's function originate from the denominator whose zeros can be interpreted as single-particle excitations. If the Green's function has a pole $\omega_{\boldsymbol{k}}$ in the momentum state $\boldsymbol{k}$, then the spectral function $A^+_{\boldsymbol{k}}(\omega)$ will have a strong maximum at the energy $\omega_{\boldsymbol{k}} = \omega - \mu$. If $c^+_{\boldsymbol{k}}|N\rangle$ was an eigenstate, the peak would be a δ-function. In the presence of an interaction, the state $c^+_{\boldsymbol{k}}|N\rangle$ will not be, in general, an eigenstate. The system will have many other states with the same momentum. An exact eigenstate will be a linear combination of the respective Slater determinants with energies spread out by the interaction. The shape of the function $A^+_{\boldsymbol{k}}(\omega)$ will depend strongly on the interaction: the stronger the interaction the larger the spread of energies and hence the larger the width of the function $A^+_{\boldsymbol{k}}(\omega)$. Inserting the spectral functions back into the time-representation of the Green's function, one sees that a finite width of the spectral function gives rise to a loss of coherence with increasing time, and hence to a damping of the propagation. The behaviour for positive times will be approximately:

$$iG_{\boldsymbol{k}}(t) \sim z_{\boldsymbol{k}} e^{-i\omega_{\boldsymbol{k}}t - \Gamma_{\boldsymbol{k}}t} + iG^{\text{incoherent}}_{\boldsymbol{k}}(t), \quad \Gamma_{\boldsymbol{k}} > 0, \;\; t > 0 \quad (3.32)$$

where $\omega_{\boldsymbol{k}}$ defines the quasi-particle energy, $\Gamma_{\boldsymbol{k}}$ the quasi-particle inverse lifetime. The factor $z_{\boldsymbol{k}}$ is called the quasi-particle weight and describes the amount of coherence in the quasi-particle Green's function.

The above quasi-particle Green's function reads in frequency space:

$$G_{\boldsymbol{k}}(\omega) = \frac{z_{\boldsymbol{k}}}{\omega - \omega_{\boldsymbol{k}} + i\Gamma_{\boldsymbol{k}}} + G_{\boldsymbol{k}}^{\text{incoherent}}(\omega), \quad \omega > \mu, \tag{3.33}$$

Now, in contrast to (3.26), $\Gamma_{\boldsymbol{k}}$ is finite because it is determined by the interactions. The incoherent part of the Green's function is a smooth and mainly structureless function of frequency. This form gives rise to the spectral function

$$A_{\boldsymbol{k}}^{+}(\omega) \sim \left| \frac{\mathrm{Re}z_{\boldsymbol{k}} + \mathrm{Im}z_{\boldsymbol{k}}(\omega - \omega_{\boldsymbol{k}})}{(\omega - \omega_{\boldsymbol{k}}) + \Gamma_{\boldsymbol{k}}^2} \right|. \tag{3.34}$$

The last equation shows that the shape of $A_{\boldsymbol{k}}^{+}(\omega)$ is determined by the pole in the complex plane, and in the special case, $\mathrm{Im}z_{\boldsymbol{k}} = 0$, it has the symmetric Lorentzian form. In general, the spectral function has the asymmetric Breit-Wigner shape as illustrated in Fig. 3.1. The peak in $A_{\boldsymbol{k}}^{+}(\omega)$ is associated with a quasi-particle state or elementary excitation. The physical meaning of $\Gamma_{\boldsymbol{k}}$ is clearly seen from the time-representation (3.33).

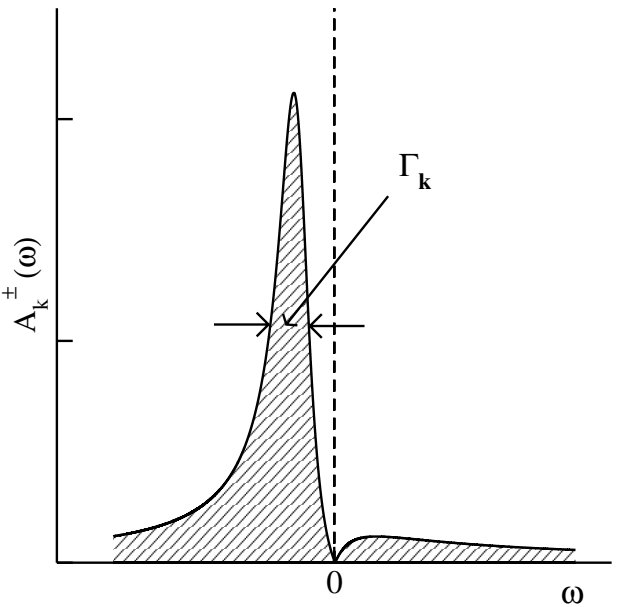

Fig. 3.1. Spectral functions $A_{\boldsymbol{k}}^{\pm}(\omega)$ with a quasi-particle peak of energy $\omega_{\boldsymbol{k}} > \mu$ with lifetime $\Gamma_{\boldsymbol{k}}^{-1}$.

3.1.3 Self-Energy

The exact explicit expression for the single-particle Green's function or its spectral function is only known for a few systems. In general one has to resort to some approximations for the Green's function. One class of approximations is derived via the equation of motion (3.19). It is useful to split the Hamiltonian into its non-interacting part $\hat{H}_0$, which now also includes the Coulomb potential from the electron charge density, and the interaction $\hat{V}$. Application of these equations to the definition of the Green's function leads to the equation of motion for the single-particle Green's function

$$\begin{aligned}&\left[i\frac{\partial}{\partial t} - \hat{H}_0\right] G_{\sigma,\sigma'}(\boldsymbol{r}\,t, \boldsymbol{r}'t') \\ &\quad + i\int \mathrm{d}^3 r'' v(\boldsymbol{r}, \boldsymbol{r}'') \langle \Psi_0 | T\left[\hat{\Psi}^+_{\sigma''}(\boldsymbol{r}''t)\hat{\Psi}_{\sigma''}(\boldsymbol{r}''t)\hat{\Psi}_{\sigma}(\boldsymbol{r}t)\hat{\Psi}^+_{\sigma'}(\boldsymbol{r}'t')\right] |\Psi_0\rangle \\ &= \delta(\boldsymbol{r} - \boldsymbol{r'})\delta_{\sigma,\sigma'}\delta(t - t'). \end{aligned} \tag{3.35}$$

where

$$v(\boldsymbol{r}, \boldsymbol{r}') = \frac{1}{|\boldsymbol{r} - \boldsymbol{r}'|} \tag{3.36}$$

is the Coulomb kernel. This equation involves a two-particle Green's function. The equation of motion of the two-particle Green's function contains the three-particle Green's function, and so on. Subsequent application of 3.20 generates a hierarchy of equations, which relate an n-body Green's function to an n+1 body Green's function. Approximations can be obtained when this hierarchy is truncated at some stage by making an decoupling ansatz for higher order Green's functions in terms of lower order Green's functions.

An alternative approach is to define a generalized, non-local and energy-dependent potential, which formally includes all effects due to the interaction. The equation

$$\begin{aligned}&\left[i\frac{\partial}{\partial t} - \hat{H}_0\right] G_{\sigma,\sigma'}(\boldsymbol{r}\,t, \boldsymbol{r}'t') \\ &\quad - \sum_{\sigma''} \int \mathrm{d}^3 r'' \int \mathrm{d}t'' \Sigma_{\sigma,\sigma''}(\boldsymbol{r}\,t, \boldsymbol{r}''t'')\, G_{\sigma''\sigma 1'}(\boldsymbol{r}''t'', \boldsymbol{r}'t') \\ &= \delta_{\sigma,\sigma'}\delta(\boldsymbol{r} - \boldsymbol{r'})\delta(t - t') \end{aligned} \tag{3.37}$$

implicitly defines this potential $\Sigma_{\sigma,\sigma''}(\boldsymbol{r}t, \boldsymbol{r}''t'')$, which is called the self-energy operator, or mass operator.

Introducing the Green's function of the non-interacting part of the Hamiltonian, $\hat{H}_0$, which obeys the equation

$$\left[i\frac{\partial}{\partial t} - \hat{H}_0\right] G^0_{\sigma,\sigma'}(\boldsymbol{r}\,t, \boldsymbol{r}'t') = \delta(\boldsymbol{r} - \boldsymbol{r'})\delta_{\sigma,\sigma'}\delta(t - t') \tag{3.38}$$

one easily sees that the full and the non-interacting Green's function are related by the Dyson equation:

$$G_{\sigma,\sigma'}(\boldsymbol{r},\boldsymbol{r}';\omega) = G^0_{\sigma,\sigma'}(\boldsymbol{r},\boldsymbol{r}';\omega) + \int \mathrm{d}^3x \int \mathrm{d}^3x' \sum_{\sigma_1.\sigma_2} G^0_{\sigma,\sigma_1}(\boldsymbol{r},\boldsymbol{x};\omega)\, \Sigma_{\sigma_1,\sigma_2}(\boldsymbol{x},\boldsymbol{x}';\omega) G_{\sigma_2,\sigma'}(\boldsymbol{x}',\boldsymbol{r}';\omega). \quad (3.39)$$

The Dyson equation can also be derived using Feynman's diagrammatic technique. More details about that can be found in standard text books on the many-body problem [3.22, 3.24, 3.42].

The simplest approximation for the self-energy is the complete neglect of it, i.e.

$$\Sigma \equiv \Sigma_H = 0, \quad (3.40)$$

corresponding to the case of $\hat{V} = 0$. Since the classical electrostatic potential is already included in H_0 this reduces to the Hartree approximation to the many-body problem. Due to the structure of the Dyson equation an approximation for the self-energy of finite order corresponds to an infinite order perturbation theory. The self-energy can be evaluated by using Wick's theorem, Feynman's diagram technique or by Schwinger's functional derivative method.

Here we follow Hedin and Lundquist [3.29] and present an iterative method for generating more and more elaborate approximations to the self-energy. The self-energy is a functional of the full Green's function and can formally also be expressed as a series expansion in a dynamically screened interaction W. In turn, the screened Coulomb interaction can be expressed via the polarisation function P which is related to the dielectric function. One can show that all functions appearing in the evaluation of the full Green's function and the self-energy, form a set of coupled integral equations which are known as the Hedin equations. Here we present this set of equations, as common in literature, in the real-space/time representation

$$G(1,2) = G_0(1,2) + \int d(3,4) G_0(1,3) \Sigma(3,4) G(4,2), \quad (3.41)$$

$$\Sigma(1,2) = i \int d(3,4) W(1,3^+) G(1,4) \Gamma(4,2;3), \quad (3.42)$$

$$W(1,2) = v(1,2) + \int d(3,4) v(1,3) P(3,4) W(4,2), \quad (3.43)$$

$$P(1,2) = -i \int d(3,4) G(2,3) \Gamma(3,4;1) G(4,2^+), \quad (3.44)$$

$$\Gamma(1,2;3) = \delta(1-2)\delta(2-3) + \int d(4,5,6,7) \frac{\delta \Sigma(1,2)}{\delta G(4,5)} G(4,6) G(7,5) \Gamma(6,7;3), \quad (3.45)$$

where we have used an abbreviated notation $(1) = (\boldsymbol{r}_1, \sigma_1, t_1)$ (the symbol t^+ means $\lim \eta \to 0(t+\eta)$ where η is a positive real number). $v(1,2) = v(\boldsymbol{r}, \boldsymbol{r}')\delta(t_1 - t_2)$ is the bare Coulomb potential, and $\Gamma(1,2;3)$ is the vertex function containing fluctuations of the charge density. The Hedin equations should be solved self-consistently: one starts with $\Sigma = 0$ in (3.45), then one calculates, with some starting Green's function, the polarisation function (3.44), the screened Coulomb function (3.43), the self-energy (3.42), and finally, with the Dyson equation (3.41), the new Green's function which should be used with the self-energy for evaluation of the vertex function (3.45). This process should be repeated until the resulting Green's function coincides with the starting one. For real materials such calculations are extremely difficult, mainly because of the complexity of the vertex function (3.45). In practice one usually truncates the self-consistency cycle and approximates one or more functions, appearing in the Hedin equations (3.41)-(3.45).

Before we turn to practical approaches for the self energy, we shall consider its characteristic features following from quite general considerations [3.39].

The formal solution of Dyson's equation (for translational invariant systems in momentum space) is:

$$G_{\boldsymbol{k}}(\omega) = \frac{1}{\omega - \omega^0_{\boldsymbol{k}} - \Sigma_{\boldsymbol{k}}(\omega)}. \tag{3.46}$$

The singularities of the exact Green's function $G_{\boldsymbol{k}}(\omega)$, considered as a function of ω, determine both the excitation energies $\omega_{\boldsymbol{k}}$ of the system and their damping $\Gamma_{\boldsymbol{k}}$. From the Lehman representation (3.30) and the Dyson equation (3.46) it follows that the excitation energy $\omega_{\boldsymbol{k}}$ is given by

$$\omega_{\boldsymbol{k}} = \omega^0_{\boldsymbol{k}} + \mathrm{Re}\Sigma_{\boldsymbol{k}}(\omega_{\boldsymbol{k}}). \tag{3.47}$$

Analogously, the damping $\Gamma_{\boldsymbol{k}}$ is defined by the imaginary part of the self-energy:

$$\Gamma_{\boldsymbol{k}} = [1 - \frac{\partial \mathrm{Re}\Sigma_{\boldsymbol{k}}(\omega_{\boldsymbol{k}})}{\partial \omega}]^{-1} \mathrm{Im}\Sigma_{\boldsymbol{k}}(\omega_{\boldsymbol{k}}). \tag{3.48}$$

Using the behaviour of the Green's function for large $|\omega|$, we can write an assymtotic series

$$[G_{\boldsymbol{k}}(\omega)]^{-1} = \omega + a_{\boldsymbol{k}} + b_{\boldsymbol{k}}/\omega + ..., \tag{3.49}$$

and from (3.46) it follows that the self-energy is a regular function at infinity:

$$\Sigma_{\boldsymbol{k}}(\omega) = -(\omega^0_{\boldsymbol{k}} + a_{\boldsymbol{k}} + b_{\boldsymbol{k}}/\omega + ...) \tag{3.50}$$

Further, since the imaginary part of the Green's function never vanishes except on the real axis, the Green's function $G_{\boldsymbol{k}}(\omega)$ has no complex zeros. From

the analyticity of $G_{\boldsymbol{k}}(\omega)$ it follows that $\Sigma_{\boldsymbol{k}}(\omega)$ is analytic everywhere in the complex plane with the possible exception of the real axis. Another important property of the self-energy is its behaviour in the vicinity of the chemical potential. If one finds

$$|\mathrm{Im}\Sigma_{\boldsymbol{k}}(\omega)| \sim (\omega - \mu)^2 \tag{3.51}$$

then the system is called a Fermi liquid [3.40]. This relation is not valid in general because one of its consequences is the existence of a sharp Fermi surface, which is certainly not present in some systems of fermions with attractive forces between particles.

3.1.4 Kohn-Sham Approximation for the Self-Energy

In the last section we have discussed general properties of the Green's function and how the Green's function is related to quasi-particle excitations. Now we shall consider some practical approaches for the self-energy, with which we can solve the Dyson equation (3.39) on a first-principles (or ab-initio) level.

The first method we discuss is the direct application of density functional theory (DFT) to the calculation of the Green's function.

DFT is one of the most powerful and widely used ab-initio methods [3.14, 3.19, 3.45]. It is based on the Hohenberg and Kohn theorem [3.30], which implies, that all ground state properties of an inhomogeneous electron gas can be described by a functional of the electron density, and provides a one-to-one mapping between the ground-state density and the external potential. Kohn and Sham [3.34] used the fact that this one-to-one mapping holds both for an interacting and a non-interacting system, to define an effective, non-interacting system, which yields the same ground-state density as the interacting system. The total energy can be expressed in terms of this non-interacting auxiliary system as:

$$E_0 = \min_{\rho} \left\{ T[\rho] + \int v_{\mathrm{ext}}(\boldsymbol{r})\rho(\boldsymbol{r})\mathrm{d}^3r + \frac{1}{2}\int\int \frac{\rho(\boldsymbol{r})\rho(\boldsymbol{r}')}{|\boldsymbol{r}-\boldsymbol{r}'|}\mathrm{d}^3r\mathrm{d}^3r' + \right.$$
$$\left. + E_{xc}[\rho] \right\} . \tag{3.52}$$

Here the first term is kinetic energy of a non-interacting system with the density ρ, the second one is the potential energy of the external field $v_{\mathrm{ext}}(\boldsymbol{r})$, the third is the Hartree energy, and the exchange-correlation energy $E_{xc}[\rho]$ entails all interactions, which are not included in the previous terms. The charge density $\rho(\boldsymbol{r})$ of the non-interacting system, which by construction equals the charge density of the full system, can be expressed through the orthogonal and normalized functions $\varphi_i(\boldsymbol{r})$ as

$$\rho(\boldsymbol{r}) = \sum_{i}^{\mathrm{occ.}} |\varphi_i(\boldsymbol{r})|^2. \tag{3.53}$$

Variation of the total energy functional (3.52) with respect to the function $\varphi_i(\boldsymbol{r})$ yields a set of equations, the Kohn-Sham (KS) equations, which have to be solved self-consistently, and which are of the form of a single-particle Schrödinger equation:

$$\left[-\frac{\nabla^2}{2} + v_{\text{eff}}(\boldsymbol{r})\right] \varphi_i(\boldsymbol{r}) = \varepsilon_i \varphi_i(\boldsymbol{r}). \tag{3.54}$$

This scheme corresponds to a single-particle problem, in which electrons move in the effective potential

$$v_{\text{eff}}(\boldsymbol{r}) = v_{\text{ext}}(\boldsymbol{r}) + v_{\text{H}}(\boldsymbol{r}) + v_{\text{xc}}(\boldsymbol{r}). \tag{3.55}$$

Here $v_{\text{H}}(\boldsymbol{r})$ is the Hartree potential and $v_{\text{xc}}(\boldsymbol{r}) = \frac{\delta E_{\text{xc}}(\rho(\boldsymbol{r}))}{\delta \rho(\boldsymbol{r})}$ is the exchange-correlation potential.

The energy functional (3.52) provides in principle the exact ground state energy if the exchange-correlation energy $E_{xc}[\rho]$ is known exactly. This functional is difficult to find, since this would be equivalent to the solution of the many-body problem, and remains a topic of current research in density-functional theory. For applications the exchange-correlation energy $E_{xc}[\rho]$ is usually approximated by some known functionals obtained from some simpler model systems. One of the most popular approaches is the local-density approximation (LDA), in which the exchange-correlation energy $E_{xc}[\rho]$ of an inhomogeneous system is approximated by the exchange-correlation energy of a homogeneous electron gas, which can be evaluated accurately, e.g., by Quantum Monte Carlo techniques. Thereby all many-body effects are included on the level of the homogeneous electron gas in the local exchange-correlation potential, which depends on the electronic density and some parameters obtained from many-body calculations for a the homogeneous electron gas [3.57, 3.13, 3.58, 3.48, 3.47]. In many cases the LDA works well and is already for three decades widely used for great variety of systems (see review by R.O. Jones and O. Gunnarsson [3.31], and some text books on DFT [3.14, 3.19, 3.45]). The simplicity of the local density approximation makes it possible to solve the Kohn-Sham equation (3.54) with different basis sets and for different symmetry cases. When the on-site Coulomb interaction dominates the behaviour of electrons (strongly correlated systems), the local-density does not work well, and another approximation of $E_{xc}[\rho]$ is needed.

As was already mentioned above, standard density functional theory is designed for the study of ground state properties. In many cases it appears reasonable to interpret the eigenvalues ε_i in the one-particle equation (3.54) as excitation energies, but there is no real justification for such an interpretation [3.46, 3.51]. However, also the Green's function and thus the self-energy are, among other dependencies, functionals of the electronic density. Sham and Kohn argue that for sufficiently homogenous systems, and for energies in the close vicinity of the Fermi-surface, the approximation

$$\Sigma(\boldsymbol{r},\boldsymbol{r}';\omega) \approx v_{xc}[\rho](\boldsymbol{r})\delta(\boldsymbol{r}-\boldsymbol{r}') \tag{3.56}$$

should be good. The range of energies, in which this approximation can be expected to work, depends on the effective mass of a homogeneous electron gas with a density, corresponding to some average of the actual density of the system. Using this approximation in the Dyson equation, one sees that the full Green's function is approximated by the Green's function of the non-interacting Kohn-Sham system, which can be expressed in terms of the KS orbitals and KS energies:

$$G_{\mathrm{KS},\sigma,\sigma'}(\boldsymbol{r},\boldsymbol{r}';\omega) = \lim_{\Gamma\to 0}\left(\sum_i^{\mathrm{occ}} \frac{\varphi_{i\sigma}(\boldsymbol{r})\varphi^*_{i\sigma'}(\boldsymbol{r}')}{\omega-\mu+\epsilon_i+i\Gamma} + \sum_i^{\mathrm{unocc}} \frac{\varphi_{i\sigma}(\boldsymbol{r})\varphi^*_{i\sigma'}(\boldsymbol{r}')}{\omega-\mu+\epsilon_i-i\Gamma}\right) \tag{3.57}$$

This argument explains why the otherwise unjustified interpretation of the Kohn-Sham Green's function, often gives surprisingly good results for spectroscopy calculations. Despite the lack of a proper justification, this fact led to the development of variety of methods on the first-principle level, which are successfully applied for many spectroscopy phenomena (see recent reviews in [3.16, 3.15]). An example, how the density functional theory within the LDA does work, is illustrated in Fig. 3.2. Here we present magneto-optical spectra for iron calculated by a self-consistent LMTO method [3.3] and the experimental results [3.37]. Because magneto-optics in the visible light belongs to the low-energy spectroscopy, one can expect, that the use of the LDA is reasonable. Indeed, the calculated polar Kerr rotation and Kerr ellipticity agree very well with the experimental curve. The theoretical curve reproduces all main features of the experimental result. With increasing energy the agreement with experiment is getting worse, as expected from the deterioration of the LDA approximation for higher energies. The theory also could not represent the magnitude of the experimental curve for the whole energy range; this is related to the damping of the quasi-particle states. The main failure of the LDA in the description of spectroscopic phenomena is the inability to reproduce the damping of single-particle excitation, which is given by the imaginary part of the self-energy (3.48) and which is not present in the approximation (3.81). The calculated spectrum is usually artificially smeared by a Lorentzian broadening with some constant width Γ, but this is not a satisfactory approximation, because in reality the damping has a more complicated structure. An evident case when the LDA does not work is shown in Fig. 3.3. Here we present photoemission spectra for silver at a photon energy of 26 eV. The solid line shows a theoretical spectrum calculated by these authors using a self-consistent Green's function method [3.18,3.38] within the LDA. The dashed line reproduces the experiment [3.43]. The low energy part of the spectra (up to 5.5 eV below the Fermi level) is adequately represented by theory. At the energy 5.1 eV below the Fermi level the experiment shows a peak corresponding to a 4*d*-state, which is predicted by theory at 3.6 eV

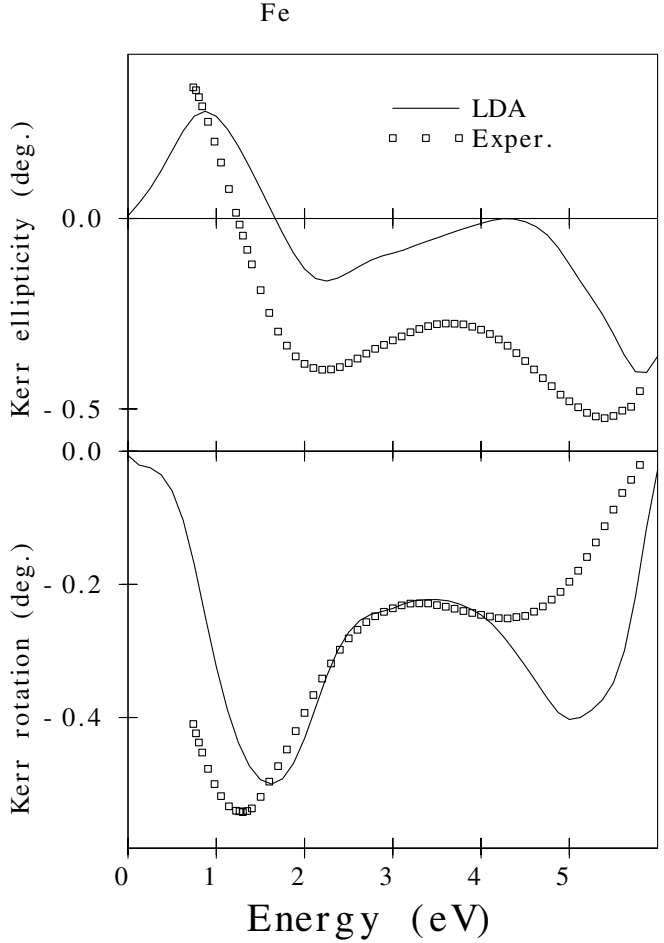

Fig. 3.2. Calculated [3.3] and experimental [3.37] magneto-optical spectra of Fe

below the Fermi level. The discrepancies are related to the inadequacy of the local approximation of $v_{xc}(r)$ and to the failure of correlating Kohn-Sham eigenvalues with excitation energies in the photoemission experiment. Below we point some serious faults of the DFT and the LDA in the description of ground state and quasi-particle state properties:

– The approximation of the exchange-correlation energy is a crucial point of DFT calculations. Existing approximations are usually not applicable for systems with partially filled inner shells. In presence of strong-correlated electrons the LDA does not provide reasonable results.
– The LDA is not completely self-interaction free. The unphysical interaction of an electron with itself can approximately be subtracted if the electron is sufficiently localized [3.48]. This remarkably improves the total energy and

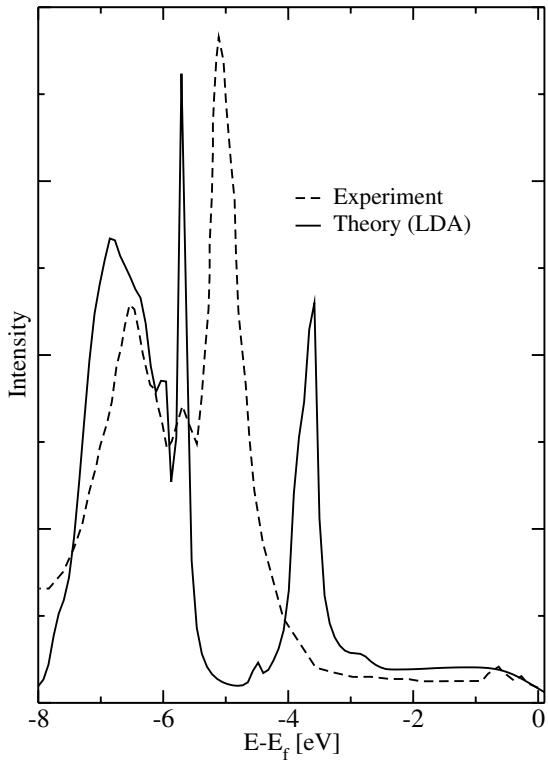

Fig. 3.3. Photoemission spectra of silver at a photon energy of 26 eV: theory (solid line) and experiment (dashed line) [3.43]

other ground state properties, but quasi-particle excitations are still badly described because the Kohn-Sham approach (3.81) is even less appropriate for strongly localized electrons. Application the SIC method for extended systems is difficult since the correction term, as proposed by Perdew and Zunger [3.48] disappears for delocalized electrons. The method can be generalized by applying the correction to localized Wannier states [3.54, 3.53].

– The band gaps in *sp*-semiconductors like Si, GaAs, Ge, etc. are by 70-100% systematically underestimated.
– The damping of excitation states can not be conceptually described within a direct interpretation of the Kohn-Sham system.

The main reason for all those problems is the fact, that (standard) density functional theory is not designed for excited states. The approximation (3.81) is empirically right only for specific materials and for a limited range of energies. Optical excitations (two-particle excitations) can, in principle, be obtained from time-dependent DFT [3.49, 3.44].

3.2 Methods of Solving the Kohn-Sham Equation

In this chapter we describe two methods of calculating the electronic band structures of crystals, which is equivalent to calculating the KS Green's function. These methods represent two general approaches of solving the Kohn-Sham equation.

In the first approach the Kohn-Sham equation can be solved in some basis set. The wave function $\varphi_i(\boldsymbol{r})$ in the Kohn-Sham equation (3.54) can be represented as linear combination of N appropriate basis functions $\phi_i(\boldsymbol{r})$:

$$\varphi(\boldsymbol{r}) = \sum_{i}^{N} C_i \phi_i(\boldsymbol{r}) \tag{3.58}$$

The basis set $\{\phi_i(\boldsymbol{r})\}$ should correspond to the specifics of the solving problem such as the crystal symmetry, the accuracy or special features of the electronic structures. According to the variational principle the differential equation (3.54) represented in the basis (3.58) can be transformed to a set of linear equations:

$$\sum_{j}^{N} (H_{ij} - \varepsilon S_{ij}) C_j = 0, \;\; j = 1, 2, .., N\,. \tag{3.59}$$

The matrices

$$H_{ij} = \int \mathrm{d}^3 r \phi_i^*(\boldsymbol{r}) \hat{H}(\boldsymbol{r}) \phi_i(\boldsymbol{r}), \tag{3.60}$$

$$S_{ij} = \int \mathrm{d}^3 r \phi_i^*(\boldsymbol{r}) \phi_i(\boldsymbol{r}) \tag{3.61}$$

are the Hamiltionan and overlap matrices respectively. Using identity

$$S = \left(S^{1/2}\right)^T S^{1/2} \tag{3.62}$$

the system of (3.59) can be easily transformed to the ordinary eigenvalue problem

$$\sum_{j}^{N} (\tilde{H}_{ij} - \varepsilon \delta_{ij}) \tilde{C}_j = 0 \tag{3.63}$$

with $\tilde{H} = \left(S^{1/2}\right)^T H S^{1/2}$ and $\tilde{C} = S^{1/2} C$. This ordinary eigenvalue problem (3.63) can by solved by the diagonalization of the matrix $\tilde{H}$.

All variational methods differ from each other only by the choice of the basis functions $\{\phi_i(\boldsymbol{r})\}$ and by the construction of the crystal potential. Several efficient basis methods have been developed in last four decades

and are widely used for band structure calculations of solids. A designated choice of basis functions serves for specific purposes. For example the *linearized muffin-tin orbital* (LMTO) method [3.1] or *augmented spherical wave* (ASW) [3.60] method provide very fast band structure calculations, with an accuracy which is sufficient for many applications in solids. A *tight-binding* representation of the basis [3.21,3.2] is very useful for different models with parameters determined from band structure calculations. Usually simple basis methods are very fast but not very accurate. Methods with more complicated basis and potential constructions are appropriate for high precision electronic structure calculations (see *augmented plane wave* (APW) method [3.52], *full-potential linearized augmented plane wave* (FPLAPW) method [3.10], *projected augmented wave* (PAW) method [3.12], *full-potential local-orbital minimum-basis* method [3.32], several norm-conserving pseudopotential methods [3.26, 3.56]). Such methods are slower than the fast simple basis methods mentioned above, but on modern computers they are successfully applied even to extended systems like large super-cells, surfaces and interfaces.

Another efficient way to solve the the Kohn-Sham equation (3.54) is the Green's function method. This approach is based on a corresponding mathematical scheme of solving differential equations. Basically the method uses Green's function technique to transform the Schrödinger equation into an equivalent integral equation. In the crystal one can expand the crystal states in a complete set of functions which are solutions of the Schrödinger equation within the unit cell, and then determine the coefficients of the expansion by requiring that the crystal states satisfy appropriate boundary conditions. This method was proposed originally by Korringa [3.35], Kohn and Rostoker [3.33], in different though equivalent form. More details about the *Korringa-Kohn-Rostoker* (KKR) method can be found in [3.23, 3.59].

As an example of ab-initio band structure methods we shall discuss below a high precision full-potential combined basis method [3.20, 3.17], which is a flexible generalisation of the LCAO computational scheme. Before we start the discussion about this approach, we consider some general features which are typical for any basis method.

In a crystal the effective potential $v_{\text{eff}}(\boldsymbol{r})$ in the Kohn-Sham equation (3.54) is a periodic function of direct lattice vectors $\boldsymbol{R}_i$: $v_{\text{eff}}(\boldsymbol{r}+\boldsymbol{R}_i) = v_{\text{eff}}(\boldsymbol{r})$. A wave function $\varphi_n(\boldsymbol{k};\boldsymbol{r})$ satisfies the Bloch theorem:

$$\varphi_n(\boldsymbol{k};\boldsymbol{r}+\boldsymbol{R}_i) = \exp\left(i\boldsymbol{k}\cdot\boldsymbol{R}_i\right)\varphi_n(\boldsymbol{k};\boldsymbol{r}) \tag{3.64}$$

Here $\boldsymbol{k}$ is a wave vector of an electron. According to the Bloch theorem solutions of the Kohn-Sham equation (3.54) depend on the wave vector $\boldsymbol{k}$ and can generally be represented as

$$\varphi_n(\boldsymbol{k};\boldsymbol{r}) = \exp\left(i\boldsymbol{k}\cdot\boldsymbol{r}\right)u_n(\boldsymbol{k};\boldsymbol{r}), \tag{3.65}$$

where $u_n(\boldsymbol{k};\boldsymbol{r})$ is a lattice periodic function. The index n is known as the band index and occurs because for a given $\boldsymbol{k}$ there will be many independent

eigenstates. In any basis method the crystal states are expanded in a complete set of Bloch type functions. The trial wave function expanded in the basis set should be close to the true wave function in the crystal. In crystals with almost free valence electrons an appropriate basis would be plane waves while the atomic-like functions are a proper choice for systems with localized valence electrons. Different methods of band calculations can be classified depending on which of the two above approaches is followed. Pseudopotential methods or *orthogonalized plane wave* (OPW) method use plane waves or modified plane waves as the basis set. The tight-binding methods like the LMTO or LCAO are based on the second concept. There are also approaches which combine both delocalized and localized functions. The aim of these schemes is to find the best fit for true wave functions in systems which contain different types of electron states. Moreover, the true wave function changes its behaviour throughout the crystal: close to the nuclear the wave function is usually strongly localized and in the interstitial region it has more free electron character. To this class of methods belongs the very popular FPLAPW method [3.10] in which the wave functions are represented by localized functions in the *muffin-tin* sphere which are smoothly matched to plane waves in the interstitial region. Here we shall discuss another combined basis approach which is based on the LCAO scheme. In the LCAO method, originally suggested by Bloch [3.11], the atomic orbitals of the atoms (or ions) inside the unit cell are used as basic expansion set for the Bloch functions. This procedure is convenient only for low energy states because the atomic orbitals are very localized and poorly describe the wave functions in the region where the crystal potential is flat. The atomic orbitals can be optimized as suggested in [3.21]. In this approach the atomic-like functions are squeezed by an additional attractive potential. The extention of the basis functions is tuned by a parameter that can be found self-consistently [3.32]. One of the main difficulties of the LCAO scheme is an abundance of multicenter integrals, which must be performed to arrive at a reasonable accuracy of band structure calculations. This difficulty is evidently most critical for solids which have a close packed structure and therefore a great number of neighbours within a given distance. To avoid these difficulties, one usually imposes some restrictions on the basis set and, as a rule, this leads to its incompleteness, which, on the other hand, is most pressing for open structures. Completeness can be regained by adding plane waves to the LCAO's. By increasing the number of plane waves in the basis we can decrease the spatial extent of localised valence orbitals and thereby reduce the number of multi-center integrals. This provides a flexibility which goes far beyond usual pseudo potentials. Retaining some overlap between the local valence orbitals, we improve our plane-wave basis set and can receive a good converged Bloch function for both valence electrons and excited states using a relatively small number of plane waves. Orthogonalization of both LCAO's and plane waves to core states can be done before forming of Hamiltonian and overlap ma-

trices. Thus, the application of combined basis sets in the combination of LCAO's and OPW's allows efficiently to use advantages both approaches.

We have to solve the Kohn-Sham equation for the electronic states in a periodic systems

$$[-\frac{1}{2}\nabla^2 + v_{\rm eff}(\boldsymbol{r})]\,\varphi_n(\boldsymbol{k};\boldsymbol{r}) = \varepsilon_n(\boldsymbol{k})\,\varphi_n(\boldsymbol{k};\boldsymbol{r})\ . \tag{3.66}$$

Here $v_{\rm eff}$ is the effective potential (3.55). The wave function $\varphi_n(\boldsymbol{k};\boldsymbol{r})$ describes the Kohn-Sham one-electron state with the wave vector $\boldsymbol{k}$ and the band index n. Without any restriction of generality the effective potential can be split into two parts: a lattice sum of single local potentials decreasing smoothly to zero at the muffin tin radii and a smooth Fourier transformed potential which is the difference between the total effective and the local potential. Thus, the effective potential can be represented as follows

$$v_{\rm eff}(\boldsymbol{r}) = \sum_{\boldsymbol{RS}} v^{\rm loc}_{\boldsymbol{S}}(\boldsymbol{r}-\boldsymbol{R}-\boldsymbol{S}) + \sum_{\boldsymbol{G}} e^{i\boldsymbol{G}\cdot\boldsymbol{r}}\, v^{\rm ft}(\boldsymbol{G})\,, \tag{3.67}$$

where $\boldsymbol{R}$ and $\boldsymbol{G}$ are direct and reciprocal lattice vectors, and $\boldsymbol{S}$ is a site position in an unit cell. The local potential is decomposed into angular contributions and with our conditions has the form

$$v^{\rm loc}_{\boldsymbol{S}}(\boldsymbol{r}) = \begin{cases} \sum\limits_L v^{\rm loc}_{\boldsymbol{S}L}(r)\,Y_L(\hat{\boldsymbol{r}}) & :\quad r \le r_{MT} \\ 0 & :\quad r > r_{MT}\ , \end{cases} \tag{3.68}$$

where $\hat{\boldsymbol{r}}$ is a normal vector along the vector $\boldsymbol{r}$. Here $Y_L(\hat{\boldsymbol{r}})$ are spherical harmonic functions with the combined index $L = \{l, m\}$. This decomposition greatly simplifies the evaluation of the required matrix elements. One-electron wave functions are sought in the combined basis approach

$$\varphi_n(\boldsymbol{k};\boldsymbol{r}) = \sum_{\mu} A_{n\mu}(\boldsymbol{k})\,\phi_\nu(\boldsymbol{k};\boldsymbol{r}) + \sum_{\boldsymbol{G}} B_{n\boldsymbol{G}}(\boldsymbol{k})\,\phi_{\boldsymbol{G}}(\boldsymbol{k};\boldsymbol{r})\ . \tag{3.69}$$

$\varphi_\mu(\boldsymbol{k};\boldsymbol{r})$ is the Bloch sum of localised site orbitals $\phi_\mu(\boldsymbol{r}-\boldsymbol{R}-\boldsymbol{S}_\mu)$. The $\mu-$sum runs over both core and valence orbitals:$\mu = \{c, \nu\}$. The core orbital contributions in a valence state are needed to provide orthogonalization of the valence state to true core states. $\varphi_{\boldsymbol{G}}(\boldsymbol{k};\boldsymbol{r}) \sim e^{i(\boldsymbol{k}+\boldsymbol{G})\cdot\boldsymbol{r}}$ is a normalised plane wave. We use core orbital contributions and plane wave contributions seperately, and do not form orthogonalised plane waves (OPWs) at the outset.

In the basis set three types of functions are used: true core orbitals, squeezed local valence orbitals and plane waves. By our definition, true core orbitals are solutions of the Kohn-Sham equation (3.66) which have negligible nearest neighbour overlap among each other (typically less than 10^{-6}). The highest fully occupied shells of each angular momentum (e.g. $2s$ and $2p$ in aluminium, or $3s$ and $3p$ in a $3d$-metal) are treated like valence orbitals in most of our calculations, because their nearest neighbour overlap is not small

enough to be neglected, if a larger number of plane waves is included. This is usually the reason for the over-completeness breakdown of OPW expansions. The local basis function (both core and valence) can be constructed from radial functions $\xi^{\mu}_{\boldsymbol{S}nl}(r)$ which are solutions of the radial Schrödinger equation

$$\left[-\frac{1}{2r}\frac{\partial^2}{\partial r^2}r + \frac{l(l+1)}{2r^2} + v^{\mu}_{\boldsymbol{S}}(r)\right]\xi^{\mu}_{\boldsymbol{S}nl}(r) = \varepsilon^{\mu}_{\boldsymbol{S}nl}\xi^{\mu}_{\boldsymbol{S}nl}(r)\,. \tag{3.70}$$

Here, in the case of core electrons ($\mu = c$) the potential $v^{c}_{\boldsymbol{S}}(r)$ is the crystal potential averaged around the center $\boldsymbol{S}$. To obtain squeezed valence electrons ($\mu = \nu$) we use a specially prepared spherical potential by adding an artificial attractive potential to $v^{c}_{\boldsymbol{S}}(r)$:

$$v^{\nu}_{\boldsymbol{S}}(r) = v^{c}_{\boldsymbol{S}}(r) + \left(\frac{r}{r_{\nu}}\right)^4 \tag{3.71}$$

with a parameter r_{ν} which serves to tune the radial expansion of the basis functions and can be found self-consistently on the total energy minimum condition. A useful local valence basis orbital should on the contrary rapidly die off outside the atomic volume of its centre, but smooth enough for the Bloch sums of those orbitals to provide a smooth and close approximant to the true valence Bloch wave function so that the remaining difference between the two may be represented by a few OPWs. A local basis function is denoted in the following manner

$$\eta_{\mu}(\boldsymbol{r}) = \xi^{\mu}_{\boldsymbol{S}nl}(r)Y_L(\hat{\boldsymbol{r}})\,, \tag{3.72}$$

where the lower index $\mu = \{c, \nu\}$ acts as multi-index $\{\boldsymbol{S}nlm\}$ for core and valence basis functions respectively.

The third kind of basis functions are plane waves normalised to the crystal volume V:

$$\eta_{\boldsymbol{k}}(\boldsymbol{r}) = \frac{1}{\sqrt{V}}e^{i\boldsymbol{k}\cdot\boldsymbol{r}}\,,\quad V = NV_u\,, \tag{3.73}$$

where N is the number of unit cells and V_u is the unit cell volume. To summarise, the entries in the expansion (3.66) are the basis Bloch functions

$$\phi_c(\boldsymbol{k};\boldsymbol{r}) \equiv (\boldsymbol{r}|\boldsymbol{k}c) = \sum_{\boldsymbol{R}}\eta_c(\boldsymbol{r}-\boldsymbol{R}-\boldsymbol{S}_c)\frac{1}{\sqrt{N}}e^{i\boldsymbol{k}\cdot(\boldsymbol{R}+\boldsymbol{S}_c)}\,, \tag{3.74}$$

$$\phi_{\nu}(\boldsymbol{k};\boldsymbol{r}) \equiv (\boldsymbol{r}|\boldsymbol{k}\nu) = \sum_{\boldsymbol{R}}\eta_{\nu}(\boldsymbol{r}-\boldsymbol{R}-\boldsymbol{S}_{\nu})\frac{1}{\sqrt{N}}e^{i\boldsymbol{k}\cdot(\boldsymbol{R}+\boldsymbol{S}_{\nu})}\,, \tag{3.75}$$

$$\phi_{\boldsymbol{G}}(\boldsymbol{k};\boldsymbol{r}) \equiv (\boldsymbol{r}|\boldsymbol{k}\boldsymbol{G}) = \eta_{\boldsymbol{k}+\boldsymbol{G}}(\boldsymbol{r}) \tag{3.76}$$

The flexibility of the basis (3.72) and (3.73) consists in a balance between the radial extension of the valence basis orbitals and the number of plane

waves needed to converge the expansion (3.69). By reducing the parameters r_ν and/or the number of local basis orbitals, the number of multi-center integrals needed in the calculation is reduced at the price of slowing down the convergence speed with the number of plane waves included, and vice versa. Our approach provides a full interpolation between the LCAO and OPW approaches adopting pseudo-potential features.

After the expansion of the wave functions in (3.66) we have the following system of linear equations

$$\sum_{\mu} \left[(\boldsymbol{k}\mu'|H|\boldsymbol{k}\mu) - E\ (\boldsymbol{k}\mu'|\boldsymbol{k}\mu) \right] A^{\mu}(\boldsymbol{k}) = 0\,, \tag{3.77}$$

which gives us the sought band energies $E = E_n(\boldsymbol{k})\,, n = 1, ..., M$, where M gives the rank of the coefficient matrix and corresponds to the number of basis functions. For the expansion coefficients $A^{\mu}_n(\boldsymbol{k})$ there are M different solutions. The equation system poses the eigenvalue problem

$$(\mathcal{H} - E\mathcal{S})\mathcal{A} = 0 \tag{3.78}$$

with Hamilton matrix $\mathcal{H}$ and overlap matrix $\mathcal{S}$. To solve this eigenvalues problem the matrix elements of the Hamiltionan and overlap matrices must be calculated. This is a non-trivial problem because the basis consists of three types of functions. Moreover the local valence functions are extended in real space and overlap with each other and with the core orbitals. Because of this one needs to calculate multi-center integrals which are assumed to be independent of the wave vector. Due to the limited space we shall not discuss this problem in the paper and refer the reader to the literature [3.20, 3.17, 3.32] for more details. The secular equation (3.78) can be solved in the same manner as discussed in the previous paper by H. Eschrig. The orthogonality of the core orbitals allows us to restructure the matrix in (3.78) so that the eigenvalue problem will be reduced. According to this scheme the solution of the system of (3.78) can be carried out in the following manner. As the first step the matrices $\mathcal{S}_{c\lambda}$, $\mathcal{S}_{\lambda\lambda}$, $\mathcal{H}_{\lambda\lambda}$ ($\lambda = \{\nu, G\}$ is common index for valence basis functions) and the energies of core states ε_c are determined. Then the matrix

$$\mathcal{S}_{\lambda\lambda} - \mathcal{S}^{\dagger}_{c\lambda}\mathcal{S}_{c\lambda}$$

is decomposed into the product of left tridiagonal matrix $\mathcal{S}^{l}_{\lambda\lambda}$ and right tridiagonal matrix $\mathcal{S}^{l\dagger}_{\lambda\lambda}$ with the Cholesky method. The next step is the calculation of the inverse matrix $(\mathcal{S}^{l}_{\lambda\lambda})^{-1}$. Using this matrix we can calculate the matrix

$$\tilde{\mathcal{H}}_{\lambda\lambda} = \left(\mathcal{S}^{l}_{\lambda\lambda}\right)^{-1\dagger} \left[\mathcal{H}_{\lambda\lambda} - S^{\dagger}_{c\lambda}\mathcal{H}_{cc}S_{c\lambda} \right] \left(\mathcal{S}^{l}_{\lambda\lambda}\right)^{-1}\ . \tag{3.79}$$

After diagonalisation of the matrix $\tilde{\mathcal{H}}_{\lambda\lambda}$ we get the matrix $U_{\lambda\lambda}$, which diagonalizes $\tilde{\mathcal{H}}$ and with this matrix the expansion coefficients $\mathcal{A}$ can be written as:

$$\mathcal{A}^T = \begin{pmatrix} 1 & -\mathcal{S}_{c\lambda}\left(\mathcal{S}^r_{\lambda\lambda}\right)^{-1} U_{\lambda\lambda} \\ 0 & \left(\mathcal{S}^r_{\lambda\lambda}\right)^{-1} U_{\lambda\lambda} \end{pmatrix} . \tag{3.80}$$

The first column of the matrix $\mathcal{A}$ corresponds to the expansion coefficients of core states. According to our assumption that the core states are completely occupied, they do not overlap and are independent of the crystal momentum $\boldsymbol{k}$. Therefore one of the coefficients $A^c(\boldsymbol{k})$ is equal to one, and all other $A^\mu(\boldsymbol{k})$ are zero. The upper block of this column is hence a unit matrix 1 with the dimension $M_c \times M_c$, where M_c is number of the core states, and the lower block is a zero matrix. The second column represents the expansion coefficients of valence functions, where the upper block includes the orthogonalization correction of the valence states to the core states, and the dimension is equal to $M_c \times M_\lambda$. Here M_λ is the number of the valence states. The preceding scheme corresponds to the orthogonalisation corrections of the valence basis due to the core states (e.g. see [3.21]). With this representation the Bloch wave function (3.69) has a convenient form, and the estimations of the matrix elements and the charge density are substantially simplified.

After the eigenvalue problem (3.78) is solved, we can estimate the Bloch function (3.69) and the electronic charge density, which in our method is treated in the same manner as the crystal potential (3.67). This approach provides a very accurate numerical representation of the charge density and the crystal potential, which can be calculated self-consistently within the local density approximation.

As it was already mentioned above the main advantage of the combined basis method is the flexibility of the basis which allows to optimize efficiently band structure calculations without losing the high numerical accuracy. This fact is illustrated in Fig. 3.4 where the self-consistent band energy for Cu is presented. In this picture we demonstrate the convergence of the band energy with the number of plane waves in the basis. The band energies have been calculated for different parameters r_ν in (3.71) which regulates the extension of the local basis functions. The overlap between the local orbitals on different centers is getting larger with increasing the parameter r_ν. Then one needs to calculate more multi-center integrals in matrix elements of the eigenvalue matrix. For smaller r_ν the overlap is reduced but one needs more plane waves to obtained an accurate band structure. Another advantage of the method is the completeness of the basis for large energy range. In many approaches, specially in linearized methods, the basis functions are appropriate only for valence bands. This is sufficient for a study of ground state properties, but makes the methods not applicable for the spectroscopy. In the combined basis method the plane waves fit adequately the high lying bands which enables accurate calculations of spectroscopic characteristics within the local density approximation. Figure 3.5 shows an example of the band structure of Si calculated by the combined basis method. The band energies are shown along symmetry lines in the Brillouin zone. The indirected gap is 0.64 eV

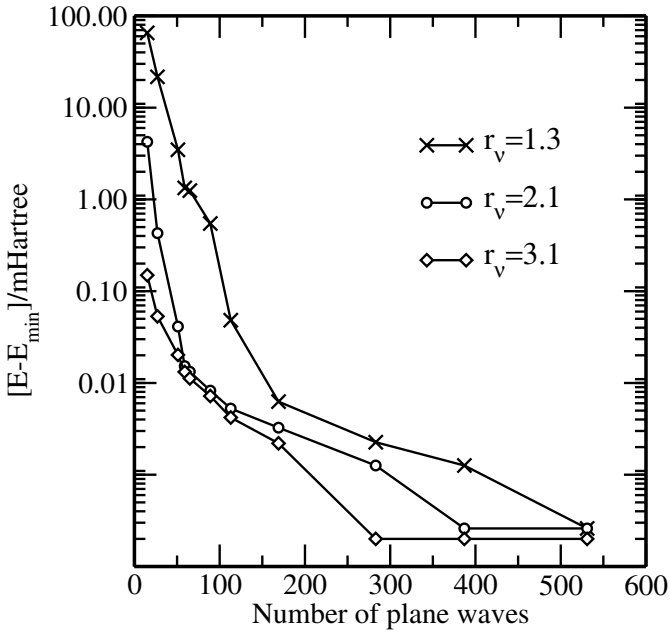

Fig. 3.4. Convergency of the self-consistent band energy of Cu for the different local basis extensions with the number of plane waves

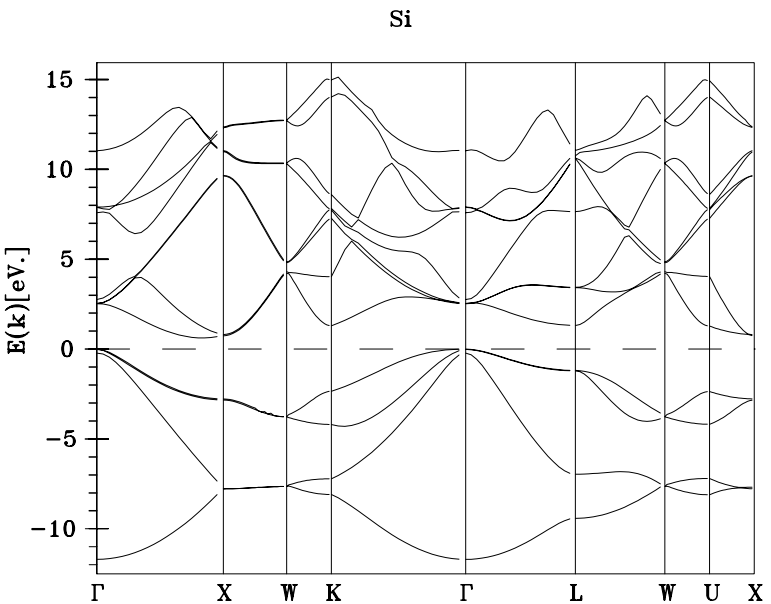

Fig. 3.5. Band structure for Si calculated with the combined basis method [3.17].

which corresponds to the expected LDA value. The band structure is in good agreement with very accurate APW and pseudo-potential calculations.

To summarize, the combined basis method is a high precision tool for the calculation of the electronic structure of solids. The basis set, consisting of localised valence orbitals and plane waves is appropriate for different types of electrons in solids. There are no shape restriction concerning both the electron density and the self-consistent potential. Typically 65 plane waves per atom yield an absolute accuracy of ≤ 1 mRyd for the total energy for a typical transition metal. Including orthogonalised plane waves into the basis set makes it possible to achieve the high precision for total energy calculations of both close packed and open systems.

3.3 GW Approximation

We shall now consider a way for approximating the self-energy using Hedin's set of (3.42)-(3.45). The most difficult part of these equations is the evaluation of the vertex function (3.45). The vertex function contains particle-hole correlation effects and is defined implicitly through the Bethe-Salpeter equation, which involves a two-particle Green's function. The functional derivative $\delta\Sigma/\delta G$ is not trivial to obtain, because the dependence of the self-energy with respect to the full Green's function is not explicitly known. If the electrons interact not too strongly, this functional derivative is small and the vertex function can be approximated by its zero order expression [3.27–3.29]:

$$\Gamma(1,2;3) \approx \delta(1-2)\delta(2-3). \tag{3.81}$$

This yields a simplified version of Hedin's set of equations:

$$\Sigma(1,2) = iW(1,2)G(1,2), \tag{3.82}$$

$$W(1,2) = v(1,2) + \int d(3,4)W(1,3)P(3,4)v(4,2), \tag{3.83}$$

$$P(1,2) = -iG(1,2)G(2,1). \tag{3.84}$$

In this approximation the self-energy is expressed as a product of the self-consistent single-particle propagator G and the self-consistent dynamically screened interaction W. This gives the name for the approximation: GW. The GW approximation (GWA) is consistent in the Baym-Kadanoff sense [3.9,3.8], i.e. it is a particle- and energy-conserving approximation. The GWA corresponds to the first iteration of the Hedin's equations and can be interpreted as the first order term of an expansion of the self-energy in terms of the screened interaction. The (3.41),(3.82)-(3.84) can be solved self-consistently, but in practice, such a calculation is computationally very expensive. Moreover, the experience with self-consistent GW implementations (see the review by F. Aryasetiawan and O. Gunnarson [3.5] and references therein)

shows that in many cases the self-consistency even worsens the results in comparison with non-self-consistent calculations. The main reason for this is the neglect the vertex correction. Most existing GW calculations do not attempt self-consistency, but determine good approximations for the single-particle propagator G and the screened interaction separately, i.e., they adopt a "best G, best W" philosophy. The common choice for the single-particle propagator is usually the LDA or Hartree-Fock Green's function. Using this Green's function the linear response function is obtained via the (3.84), and afterward it is used for the calculation of the screened Coulomb interaction (3.83). The self-energy is then determined without further iteration. Nevertheless, with the first iteration of the *GW* approximation encouraging results have been achieved. In Fig. 3.6 we show a typical result for the energy bands of MgO within the GWA (dotted line) compared to a conventional LDA calculation. It is clear from this plot that the GWA gap is in much better agreement with the experimental value than the LDA results.

Below we describe briefly some existing implementations of the GW method. More details can be found in the original papers and in the reviews [3.5, 3.7, 3.44]. The GW integral equations (3.41),(3.82)-(3.84) can be represented in some basis set in the real or reciprocal space and solved by

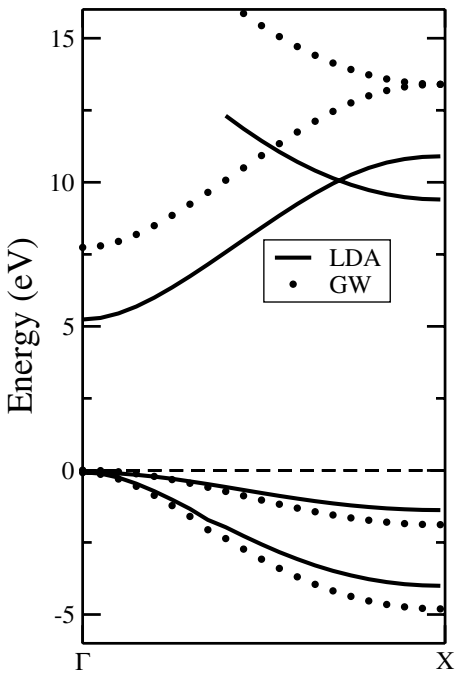

Fig. 3.6. Energy bands of MgO from KKR-LDA (solid) and GWA (dots) calculations. The LDA band gap is found to be 5.2 eV, the GWA band gap is 7.7 eV which is in good agreement with the experimental gap of 7.83 eV.

matrix inversion. The basis set should be appropriate to the symmetry of the particular problem and should be able to represent as accuratly as possible the quite distinctive behaviour of the functions, involved in the GW approach.

– *Plane wave methods*
  Pseudo-potentials in conjunction with a plane wave basis set are widely used in computational condensed matter theory due to their ease of use and their systematic convergence properties. Because of simplicity of the GW equations in the plane wave basis, the implementation of the GWA is easy, and many pseudo-potential codes contain a GW part. Conventionally a pseudo-potential method can be applied for electronic structure study of systems with delocalised *sp*-electrons for which the plane wave basis converges rapidly. But due to recent development of the pseudo-potential technique new ultra-soft pseudo-potential methods [3.56] can also be applied to materials with localised *d*- and *f*-electrons. Most of existing pseudo-potential programs are well optimised and successfully used not only for bulk-systems but also for surfaces, interfaces, defects, and clusters. A disadvantage of the plane wave basis is bad convergence for systems with localised electrons. For transition metals or f-electron systems one needs several thousand plane waves. Also the number of basis functions needed for convergence is increasing with the volume of the system. Typically a plane wave GW calculation scales with N^4, that makes calculations of extended systems very expensive.
– *The Gaussian basis method*
  Rohlfing, Krüger, and Pollman [3.41] have developed a GW method which combines a pseudo-potential basis and localised Gaussian orbitals. In this approach the LDA Green function is obtained by a conventional pseudo-potential method. Afterwards the Green's function and all GW equations are represented in localised Gaussian orbitals. This essentially reduces the size of the problem. Typically one needs 40-60 Gaussian functions. Another advantage of the method is that many of integrals can be calculated analytically. Because the pseudo-potential part is restricted for *sp*-electron compounds, the method can not be used for systems with localised electrons. A serious problem of the approach is the convergence of the Gaussian basis: while a Gaussian basis can systematically converge, the number of the basis functions needed for convergence can be quite various for different materials.
– *The linearised augmented plane wave (LAPW) method*
  The LAPW method is one of the most popular methods for the electronic structure study. The basis consists of local functions, obtained from the Schrödinger equation for atomic-like potential in a muffin-tin sphere on some radial mesh, and plane waves, which describe the interstitial region. The local functions are matched on the sphere to plane waves. Such combination of two different kinds of basis functions makes the LAPW method

extremely accurate for systems with localised or delocalised electrons. Also the plane waves are better suited for high energy states, which are usually badly represented by a conventional tight-binding method. All this makes the LAPW method attractive for the GW implementation. Hamada and coworkers developed a GW method with the LAPW [3.25] and applied it to Si. 45 basis functions per Si atom were needed which corresponds to a reduction by factor of five compared to plane wave calculations. But the computational afford is comparable with the pseudo-potential calculations because the evaluation of matrix elements is more expensive. Although a GW-LAPW realisation was successfully used also for Ni [3.4], the method did not become very popular because of the computational costs. With further development of computer technology this method may become very promising, as it was shown recently by Usuda and coworkers [3.55] in the GW-LAPW study in wurtzite ZnO.

– *The linearised muffin-tin orbitals (LMTO) method*
The LMTO is an all-electron method [3.1,3.2] in which the wave functions are expanded as follows,

$$\psi_{n\boldsymbol{k}} = \sum_{\boldsymbol{R}L} \chi_{\boldsymbol{R}L}(\boldsymbol{r};\boldsymbol{k}) b_{n\boldsymbol{k}}(\boldsymbol{R}L), \tag{3.85}$$

where χ is the LMTO basis, given in the atomic sphere approximation by

$$\chi_{\boldsymbol{R}L}(\boldsymbol{r},\boldsymbol{k}) = \varphi_{\boldsymbol{R}L}(\boldsymbol{r}) + \sum_{\boldsymbol{R}'L'} \dot{\varphi}_{\boldsymbol{R}'L'}(\boldsymbol{r}) H_{\boldsymbol{R}L;\boldsymbol{R}L'}(\boldsymbol{k}). \tag{3.86}$$

Here $\varphi_{\boldsymbol{R}L}(\boldsymbol{r}) = \phi_{\boldsymbol{R}L}(r) Y_L(\hat{\boldsymbol{r}})$ is a solution to the Schrödinger equation inside a sphere centred on an atom at site $\boldsymbol{R}$ for a certain energy ϵ_ν, $\dot{\varphi}_{\boldsymbol{R}'L'}(\boldsymbol{r})$ is the energy derivative of $\varphi_{\boldsymbol{R}L}(\boldsymbol{r})$ at the energy ϵ_ν, and $H_{\boldsymbol{R}L;\boldsymbol{R}L'}(\boldsymbol{k})$ are the so-called LMTO structure constants. An advantage of the LMTO is that the basis functions do not depend on $\boldsymbol{k}$. The LMTO method is characterised by high computational speed, requirement of a minimal basis set (typically 9-16 orbitals per an atom), and good accuracy in the low energy range.
Aryasetiawan and Gunnarsson suggested to use a combination of the LMTO basis functions for solving the GW equations [3.6]. They showed that a set of products $\phi\phi$, $\phi\dot{\phi}$, and $\dot{\phi}\dot{\phi}$ forms a complete basis for the polarisation function (3.84) and the self-energy (3.82). This scheme allows accurate description of systems with any kinds of electrons typically with 60-100 product functions. A disadvantage of the approach is a bad representation of high energy states in the LMTO method, which are important for calculations of the polarisation function and the self-energy. Recently, Kotani and van Schilfgaarde developed a full-potential version of the LMTO product basis method [3.36], with an accuracy which is substantially better than that of the conventional GW-LMTO implementation.

– *The spacetime method*
Most of the existing implementations of the GWA are in the real fre-

quency / reciprocal space representation. In this approach the evaluation of the linear response function

$$P_{\boldsymbol{q}}(\omega) = -\frac{i}{(2\pi)^4} \int\limits_{-\infty}^{\infty} \mathrm{d}\varepsilon \int\limits_{\Omega_{BZ}} \mathrm{d}^3k G^{LDA}_{\boldsymbol{k}}(\varepsilon) G^{LDA}_{\boldsymbol{k}-\boldsymbol{q}}(\varepsilon - \omega) \tag{3.87}$$

and the self-energy

$$\Sigma_{\boldsymbol{q}}(\omega) = \frac{i}{(2\pi)^4} \int\limits_{-\infty}^{\infty} \mathrm{d}\varepsilon \int\limits_{\Omega_{BZ}} \mathrm{d}^3k W_{\boldsymbol{k}}(\varepsilon) G^{LDA}_{\boldsymbol{k}-\boldsymbol{q}}(\varepsilon - \omega) \tag{3.88}$$

involves very expensive convolutions. In the real-space/time representation both functions are simple products (3.84) and (3.82), which eliminates two convolutions in reciprocal and frequency space. The idea to chose different representations to minimise the computations is realized in the spacetime method [3.50]. In this scheme the LDA wave functions $\Phi_{n\boldsymbol{k}}(\boldsymbol{r})$ are calculated with a pseudo-potential method. Then the non-interacting Green's function is analytically continuated from real to imaginary frequencies and Fourier transformed into the imaginary time:

$$G^{\mathrm{LDA}}(\boldsymbol{r}, \boldsymbol{r}'; i\tau) = \begin{cases} i \sum\limits_{n\boldsymbol{k}}^{\mathrm{occ.}} \Phi_{n\boldsymbol{k}}(\boldsymbol{r}) \Phi^*_{n\boldsymbol{k}}(\boldsymbol{r}') e^{\varepsilon_{n\boldsymbol{k}}\tau}, & \tau > 0 \\ -i \sum\limits_{n\boldsymbol{k}}^{\mathrm{unocc.}} \Phi_{n\boldsymbol{k}}(\boldsymbol{r}) \Phi^*_{n\boldsymbol{k}}(\boldsymbol{r}') e^{\varepsilon_{n\boldsymbol{k}}\tau}, & \tau < 0 \end{cases} . \tag{3.89}$$

Here $\boldsymbol{r}$ denotes a point in the irreducible part of the real space unit cell while $\boldsymbol{r}'$ denotes a point in the "interaction cell" outside of which G^{LDA} is set to zero. The linear response function is calculated in the real-space and for imaginary time with the formula (3.84) and afterwards Fourier transformed from $i\tau$ to $i\omega$ and from real space to reciprocal one. The screened Coulomb interaction is evaluated as in a conventional plane wave method, and is then transformed into the real-space/imaginary time representation to obtain the self-energy according the (3.82). Further, the self-energy can be Fourier transformed into the imaginary frequency axis and reciprocal space, and analytically continuated to real frequencies. The spacetime method decreases substantially the computational time and makes the calculation of large systems accessible. A main computational problem of the spacetime method is the storage of evaluated functions (G, P, W, and Σ) in both representations.

Acknowledgements

We thank V. Dugaev and Z. Szotek for many useful discussions. A. Ernst gratefully acknowledges support from the the DFG through the Forschergruppe 404 "Oxidic Interfaces" and the National Science Foundation under Grant No. PHY99-07949.

References

[3.1] O.K. Andersen. Linear methods in band theory. *Phys. Rev. B*, 12:3060, 1975.

[3.2] O.K. Andersen and O. Jepsen. Explicit, first-principles tight-binding theory. *Phys. Rev. Lett.*, 53:2571, 1984.

[3.3] V.N. Antonov, A.Y. Perlov, A.P. Shpak, and A.N. Yaresko. Calculation of the magneto-optical properties of ferromagnetic metals using the spin-polarised relativistic lmto method. *JMMM*, 146:205, 1995.

[3.4] F. Aryasetiawan. Self-energy of ferromagnetic nickel in the gw approximation. *Phys. Rev. B*, 46:13051, 1992.

[3.5] F. Aryasetiawan and O. Gunnarson. The *GW* method. *Rep. Prog. Phys.*, 61:237, 1998.

[3.6] F. Aryasetiawan and O. Gunnarsson. Product-basis method for calculating dielectric matrices. *Phys. Rev. B*, 49:16214, 1994.

[3.7] W.G. Aulbur, L. Jönsson, and J.W. Wilkins. Quasiparticle calculations in solids. In H. Ehrenreich and F. Spaepen, editors, *Solid State Physics*, volume 54. Academic, San Diego, 2000.

[3.8] G. Baym. Self-consistent approximations in many-body systems. *Phys. Rev.*, 127:1391, 1962.

[3.9] G. Baym and L. Kadanoff. Conservation laws and correlation functions. *Phys. Rev.*, 124:287, 1961.

[3.10] P. Blaha, K. Schwarz, P. Sorantin, and S. Trickey. Full-Potential, Linearized Augmented Plane Wave Programs for Crystalline Systems. *Comp. Phys. Commun.*, 59:399, 1990.

[3.11] F. Bloch. Über die Quantenmechanik der Elektronen in Kristallgittern. *Z. Phys.*, 52:555–600, 1928.

[3.12] P.E. Blöchel. Projector augmented-wave method. *Phys. Rev. B*, 50:17953, 1994.

[3.13] D.J. Ceperley and L. Alder. Ground state of the electron gas by a stochastic method. *Phys. Rev. Lett.*, 45:566, 1980.

[3.14] R.M. Dreizler and E.K.U. Gross. *Density Functional Theory.* Springer, Berlin, 1990.

[3.15] H. Dreyssé, editor. *Electronic Structure and Physical Properties of Solids. The Uses of the LMTO Method.* Springer, Berlin, 2000.

[3.16] H. Ebert and G. Schütz, editors. *Magnetic Dichroism and Spin Polarization in Angle-Resolved Photoemission.* Number 466 in Lecture Notes in Physics. Springer, Berlin, 1996.

[3.17] A. Ernst. full-potential-*Verfahren mit einer kombinierten Basis für die elektronische Struktur.* PhD thesis, Tu Dresden, 1997.

[3.18] A. Ernst, W.M. Temmerman, Z. Szotek, M. Woods, and P.J. Durham. Real-space angle-resolved photoemission. *Phil. Mag. B*, 78:503, 1998.

[3.19] Eschrig. *The Fundamentals of Density Functional Theory.* Teubner, Stuttgart, 1996.

[3.20] H. Eschrig. Mixed basis method. In E.K.U. Gross and R.M. Dreizler, editors, *Density Funtional Theory*, page 549. Plenum Press, New York, 19.

[3.21] H. Eschrig. *Optimized LCAO Method and the Electronic Structure of extended systems.* Springer-Verlag Berlin, 1989.

[3.22] A. Fetter and J. Walecka. *Quantum Theory of Many-Particle Systems.* McGraw-Hill, New York, 1971.

[3.23] A. Gonis. *Green Functions for Ordered and Disordered Systems*, volume 4 of *Studies in Mathematical Physics*. North-Holland, Amsterdam, 1992.
[3.24] E. Gross and E. Runge. *Vielteilchentheorie*. Teubner, Stuttgart, 1986.
[3.25] N. Hamada, M. Hwang, and A.J. Freeman. Self-energy correction for the energy bands of silicon by the full-potential linearized augmented-plane-wave method: Effect of the valence-band polarization. *Phys. Rev. B*, 41:3620, 1990.
[3.26] D.R. Hamann, M. Sclüter, and C. Chiang. Norm-conserving pseudopotentials. *Phys. Rev. Lett*, 43:1494, 1979.
[3.27] L. Hedin. *Ark. Fys.*, 30:231, 1965.
[3.28] L. Hedin. New method for calculating the one-particle green's function with application to the electron-gas problem. *Phys. Rev.*, 139:A796, 1965.
[3.29] L. Hedin and S. Lundqvist. Effects of electron-electron and electron-phonon interactions on the one-electron states of solids. In F. Seitz and D. Turnbull, editors, *Solid State Physics*, volume 23. New York: Academic, 1969.
[3.30] P. Hohenberg and W. Kohn. Inhomogeneous electron gas. *Phys. Rev.*, 136:B864, 1964.
[3.31] R.O. Jones and O. Gunnarson. The density functional formalism, its applications and prospects. *Rev. Mod. Phys.*, 61:689, 1989.
[3.32] K. Koepernik and H. Eschrig. Full-potential nonorthogonal local-orbital minimum-basis band-structure scheme. *Phys. Rev. B*, 59:1743, 1999.
[3.33] W. Kohn and N. Rostoker. Solution of the Schrödinger equation in periodic lattices with an application to metallic lithium. *Phys. Rev.*, 94:1111, 1954.
[3.34] W. Kohn and L.J. Sham. Self-consistent equations including exchange and correlation effects. *Phys. Rev*, 140:A1133, 1965.
[3.35] J. Korringa. *Physica*, 13:392, 1947.
[3.36] T. Kotani and M. van Schilfgaarde. All-electron gw approximation with the mixed basis expansion based on the full-potential lmto method. *Solid State Communications*, 121:461, 2002.
[3.37] G.S. Krinchik and V.A. Artem'ev. Magneto-optical properties of ni, co, and fe in the ultraviolet, visible and infrared parts of the spectrum. *Soviet Physics JETP*, 26:1080–1968, 1968.
[3.38] M. Lüders, A. Ernst, W.M. Temmerman, Z. Szotek, and P.J. Durham. *Ab initio* angle-resolved photoemission in multiple-scattering formulation. *J. Phys.: Condens. Matt.*, 13:8587, 2001.
[3.39] J.M. Luttinger. Analytic properties of single-particle propagators for many-fermion systems. *Phys.Rev*, 121(4):942, 1961.
[3.40] J.M. Luttinger and J.C. Ward. Ground-state energy of a many-fermion system. ii. *Phys. Rev.*, 118:1417, 1960.
[3.41] P.K. M. Rohlfing and J. Pollmann. Quasiparticle band-structure calculations for c, si, ge, gaas, and sic using gaussian-orbital basis sets. *Phys. Rev. B*, 48:17791, 1993.
[3.42] R. Mattuck. *A Guide to Feynman Diagrams in the Many-Body Problem*. McGraw-Hill, New York, 1976.
[3.43] M. Milun, P. Pervan, B. Gumhalter, and D.P. Woodruff. Photoemission intensity oscillations from quantum-well states in the Ag/V(100) overlayer system. *Phys. Rev. B*, 59:5170, 1999.
[3.44] G. Onida, L. Reining, and A. Rubio. Electronic excitations: density-functional versus many-body green's-function approaches. *Reviews of Modern Physics*, 72(2):601, 2002.

[3.45] R.G. Parr and W. Yang. *Density-Functional Theory of Atoms and Molecules*. Oxford University Press, New York, 1989.
[3.46] J. Perdew. What do kohn-sham orbital energies mean? how do atoms dissociate? In R.M. Dreizler and da Providencia J., editors, *Density Functional Methods in Physics*, volume Physics 123 of *NATO ASI Series B*, page 265. Plenum, Press, New York and London, 1985.
[3.47] J.P. Perdew and Y. Wang. Accurate and simple analytic representation of the electron-gas correlation energy. *Phys. Rev. B*, 45:13 244, 1992.
[3.48] J.P. Perdew and A. Zunger. Self-interaction correction to density-functional approximations for many-electron systems. *Phys. Rev. B*, 23:5048, 1981.
[3.49] M. Petersilka, U.J. Gossmann, and E.K.U. Gross. Excitation energies from time-dependent density-functional theory. *Phys. Rev. Lett.*, 76:1212, 1996.
[3.50] H.N. Rojas, R.W. Godby, and R.J. Needs. Space-time method for ab initio calculations of self-energies and dielectric response functions of solids. *Phys. Rev. Lett.*, 74:1827, 1995.
[3.51] L.J. Sham and W. Kohn. One-particle properties of an inhomogeneous interacting electron gas. *Phys. Rev.*, 145:561, 1966.
[3.52] J.C. Slater. Damped Electron Waves in Crystals. *Phys. Rev.*, 51:840–846, 1937.
[3.53] A. Svane. Electronic structure of cerium in the self-interaction corrected local spin density approximatio. *Phys. Rev. Lett.*, 72:1248, 1996.
[3.54] Z. Szotek, W.M. Temmerman, and H. Winter. Self-interaction corrected, local spin density description of the gamma –> alpha transition in ce. *Phys. Rev. Lett.*, 72:1244, 1994.
[3.55] M. Usuda, N. Hamada, T. Kotani, and M. van Schilfgaarde. All-electron gw calculation based on the lapw method: Application to wurtzite zno. *Phys. Rev. B*, 66:125101, 2002.
[3.56] D. Vanderblit. Soft self-consistent pseudopotentials in a generalized eigenvalue formalism. *Phys. Rev. B*, 41:1990, 1990.
[3.57] U. von Barth and L. Hedin. A local exchange-correlation potential for the spin polarised case. *J. Phys. C: Sol. State Phys.*, 5:1629, 1972.
[3.58] S.H. Vosko, L. Wilk, and M. Nusair. Accurate spin-dependent electron liquid correlation energies for local spin density calculations: A critical analysis. *Can. J. Phys.*, 58:1200, 1980.
[3.59] P. Weinberger. *Electron Scattering Theory of Ordered and Disordered Matter*. Clarendon Press, Oxford, 1990.
[3.60] A.R. Williams, J. Kübler, and C.D. Gelatt. Cohesive properties of metallic compounds: Augmented-spherical-wave calculations. *Phys. Rev. B*, 19:6094, 1979.